Effect of Magnetic Shielding on Plasma Plume of the Cylindrical Hall Thrusters

IEPC-2011-175

Presented at the 32nd International Electric Propulsion Conference,
Wiesbaden • Germany
September 11 – 15, 2011

Yevgeny Raitses,[*] Jean Carlos Gayoso,[§] and Nathaniel J. Fisch[**]
Princeton Plasma Physics Laboratory, Princeton University, Princeton, NJ, 0854, USA

Abstract: The cylindrical Hall thruster with permanent magnets produces a plasma plume with an unusual halo shape of the angular ion current distribution. The addition of the magnetic shield to the thruster magnetic circuit causes the plume shape to change to a conic type with the maximum ion current at the centerline. This is a typical plume shape for conventional annular Hall thrusters and the cylindrical Hall thrusters with electromagnet coils. Plasma potential measurements revealed that without the magnetic shield, a significant part of the acceleration region (~ 50%) is located outside the permanent magnet thruster. In this outside region, the magnetic field is strong, 100-300 Gauss. The reduction of the outside magnetic field with the magnetic shield causes the acceleration region to shift inside the thruster channel. In addition to the change of the plume shape, this process is accompanied with a significant plume narrowing. Experiments with a magnetically shielded configuration of a cylindrical Hall thruster with electromagnet coils demonstrate a complex dependence of the plume shape on the magnetic field topology.

I. Introduction

The principle of operation of the cylindrical Hall thruster (CHT) is based on a closed E×B electron drift and electrostatic acceleration of non-magnetized ions in quasineutral plasma in a hybrid magneto-electrostatic trap (Fig. 1).[1] The magnetic field configuration of the CHT can be cusp-type and magnetic mirror-type. Comprehensive studies of the CHT with electromagnet coils (CHTem) are reported elsewhere.[2] It was found that for the miniaturized 100-200 W-class CHTs, the optimal magnetic field configuration is an enhanced mirror-type (the so-called direct configuration with the co-direct currents in both electromagnet coils). The highest performance parameters of this thruster were achieved when the maximum magnetic field at the mirror was ~ 1.5-2 kGauss. In these regimes, the electromagnet coils consumed 50-100 W. For the low power thruster, this additional power consumption reduces drastically the overall thruster efficiency. The use of permanent magnets instead of electromagnet coils can offer a significant reduction of both the total electric power consumption and the thruster mass.

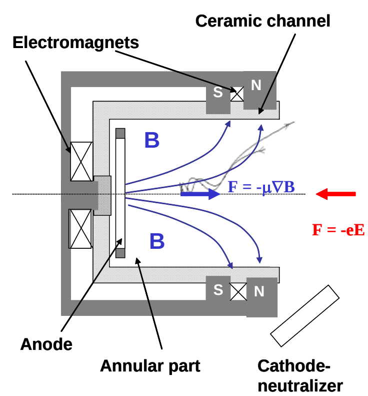

Figure 1. Schematic of a cylindrical Hall thruster (CHT).

Two permanent magnet versions of the miniaturized cylindrical Hall thruster (CHTpm) of different overall dimensions were operated in the power range of 50W-300 W.[3] The magnetic field topology of these thrusters (Fig. 2) has a magnetic mirror at the thruster center and a cusp

[*] Principal Research Physicist, Plasma Science & Technology Department, yraitses@pppl.gov
[§] Research Assistant, Plasma Science & Technology Department, jgayoso@pppl.gov
[**]Professor, Department of Astrophysical Sciences of Princeton University and PPPL, nfisch@pppl.gov

magnetic field topology near the thruster exit. For the exception of the strong magnetic field outside the CHTpm, the magnetic field topology of this thruster is similar to the magnetic field topology of its electromagnet counterpart, CHTem. The discharge and plasma plume measurements revealed that the CHT with permanent magnets and electromagnet coils operate rather differently.[3] In particular, the angular ion current density distribution from the permanent magnet thrusters has a halo shape, with a majority of high energy ions flowing at large angles with respect to the thruster centerline. It was suggested that a strong magnetic field outside the permanent magnet CHT causes these unusual characteristics of the plasma plume. Note that this halo shape of the plasma plume is also common for other types of permanent magnet cylindrical with cusped magnetic field topology, including Thales HEMP,[4] MIT's DCFT[5] and Stanford DSF thrusters.[6]

For the CHTpm thrusters, the defocusing of energetic ions could explain lower efficiencies measured for these permanent magnet thrusters as compared to the CHTem.[7] In recent experiments,[8] the magnetic shield attached to the magnetic circuit of the CHTpm was used to reduce the outside magnetic field (Fig. 2b). This modified CHTpm produced a significantly narrower plasma plume of a typical conic shape. Recent LIF measurements[9] confirmed results of probe measurements[8] that the plume from the CHTpm becomes less divergent with the magnetic shield. Performance measurements of the magnetically shielded CHTpm showed that this thruster can operate more efficient (anode efficiency of about 27-29%) than the CHTpm without the magnetic shield (~20%).[10] Moreover, the overall efficiency of the magnetically shielded CHTpm was higher than the overall efficiency of the electromagnet CHT when the power consumed by electromagnet coils is taken into account.

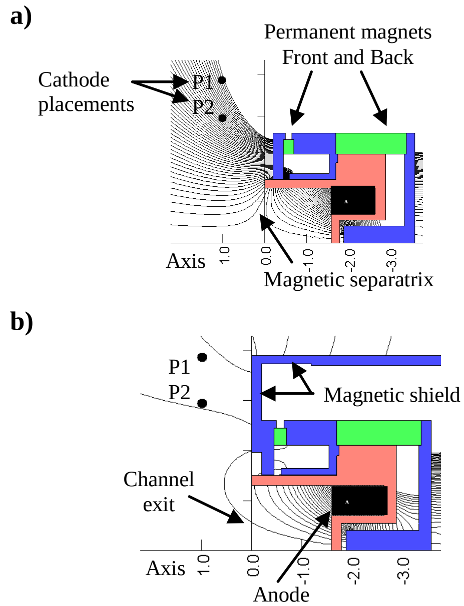

Figure 2. Magnetic field (simulations) for the the 2.6 cm diameter CHT with permanent magnets: a) without the magnetic shield,[3] $B_{zmax} \approx$ 2.5 kGauss at the magnetic mirror and (b) with the magnetic shield,[8] $B_{zmax} \approx$ 1.8 kGauss. Magnetic iron parts made from a low carbon steel are marked in blue. Samarium-cobalt permanent magnets are marked in green. Two cathode placements, P1 and P2 used in CHTpm experiments[11] are also shown. All dimensions are in cm.

For the CHTpm without the magnetic shield, the outside magnetic field links to the placement of the magnetic field separatrix with respect to the channel exit (Fig. 2a). When the magnetic field magnitude outside the CHTpm is sufficiently reduced by the magnetic shield, the magnetic separatrix moves outside the channel and starts at the magnetic shield (Fig. 2b). For this magnetically shielded CHTpm, the cathode placement with respect to the magnetic separatrix and the auxiliary cathode-keeper discharge can additionally affect to some degree the plasma plume of the CHTpm.[11] In particular, with the cathode placement at the magnetic separatrix (P2), an additional plume narrowing can be achieved by running the auxiliary cathode discharge. The cathode effect on the plume angle is, however, not as strong as the effect of the magnetic shield. Moreover, the effect of the cathode-keeper discharge on the ion accelerating efficiency of the magnetically shielded CHTpm is insignificant.[9] This is unlike the electromagnet CHT thrusters which were able to achieve higher anode efficiencies 35-40% in the anode power range of 50-200 W[12] and 150-200 W[13] with the auxiliary cathode discharge of 20-50 W (so-called current-overrun operation).

Although our previous studies pointed to a critical role of the magnetic field outside CHTpm without the magnetic shield, the ion acceleration in this region and the exact mechanism responsible for the formation of the halo plume remain unexplained. In particular, because the magnetic field in this region has a strong axial component, the formation of the axial plasma flow leading to the halo plume shape may require a strong departure of equipotentials from the magnetic field surfaces. There are also other scenarios, which could potentially explain the halo plume. For example, a combination of the electric and magnetic fields in the CHTpm might create an electron density region with a hollow profile leading to the halo shape of the plasma plume.[9] Finally, in recent LIF studies of the DCF thruster with multi-cusped magnetic field configuration, it was suggested that the ion acceleration occur mainly in the vicinity of the last magnetic separatrix, which is placed near the thruster exit.[6]

In this paper, we explore the dependence of the plasma plume on the magnetic field topology for the CHT thrusters with permanent magnets and electromagnet coils. It is shown that for both permanent magnet and electromagnet versions of the CHT, the halo shape of the plasma plume can exist only when the outside magnetic field has a sufficiently strong axial component to impede the radial electron flow from the cathode to the channel exit.

II. Magnetically shielded CHT thrusters

A typical CHT (Fig. 1) consists of a cylindrical ceramic channel, a ring-shaped anode, which serves also as a gas distributor, a magnetic core made from a low carbon steel, and electromagnet coils or permanent magnets.[14,15] Figs. 2 and 3 show results of simulations of the magnetic field for the 2.6 cm outer channel diameter CHT thrusters with permanent magnets and electromagnet coils, respectively.[4] The CHT with permanent magnets (CHTpm) uses two axially magnetized permanent magnet rings made from a Samarium-Cobalt alloy (Fig. 2). These magnet rings are incorporated into the thruster magnetic circuit. In order to implement the direct (enhanced mirror) configuration of the CHT both permanent magnet rings are placed with the same polarity. According to magnetic field simulations and measurements, a similarity between the magnetic field distributions produced with permanent magnets (Fig. 2a)

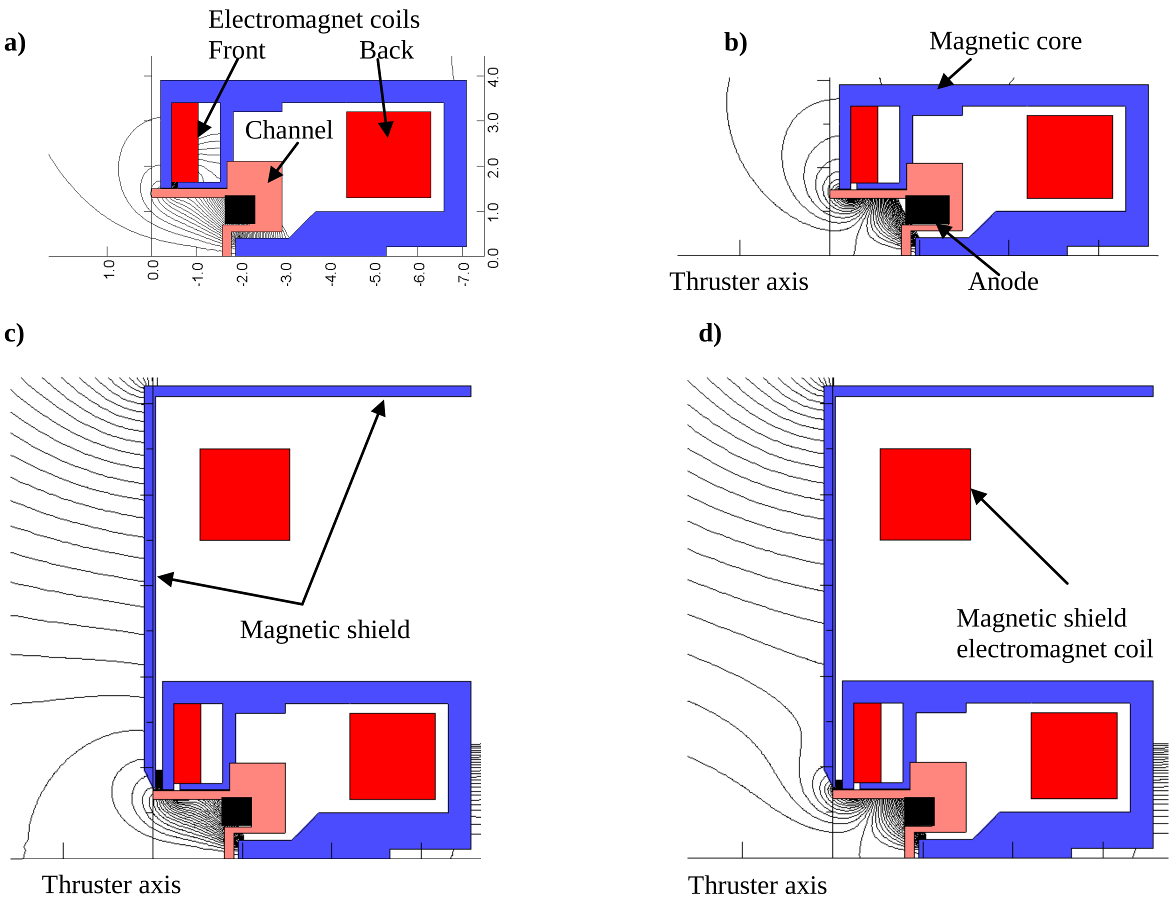

Figure 3. Magnetic field (simulations) for the direct and cusp configurations of the 2.6 cm diameter CHT with electromagnet coils ($B_{zmax} \approx$ 1.8-1.9 kGauss at the axis on the back wall) with and without the magnetic shield and the shield coil: a) the direct configuration (back coil current is 2.5 A, front coil current is 2 A) without the magnetic shield, b) the cusp configuration without the magnetic shield (back coil current is 3.2 A, front coil current is -3.2A), c) the direct configuration with the magnetic shield (back coil current is 2.5 A, front coil current is 2 A, and the shield coil current is – 4A), and d) the cusp configuration with the magnetic shield (back coil current is 2.5 A, front coil current is -2 A, and the shield coil current is – 4A). All dimensions are in cm. Magnetic iron parts are marked in blue. Electromagnet coils are marked in red. For figures b-d, major unit between mark ticks is 2 cm.

and electromagnets (Fig. 3a) exists only inside the thruster channel. However, in the vicinity of the channel exit and outside the channel, the magnetic circuit with the permanent magnets produces a different magnetic field topology. In particular, even for the direct configuration, the CHTpm has a cusped magnetic field near the channel exit (Fig. 2a). In this respect the magnetic field topology of the direct CHTpm is similar to the cusp-type configuration of the CHT with electromagnet coils (Fig. 3b). For the cusp CHTem, when the absolute value of the front coil current is above 3 A, the magnitude of the magnetic field in the cusp region inside the thruster channel is comparable to the

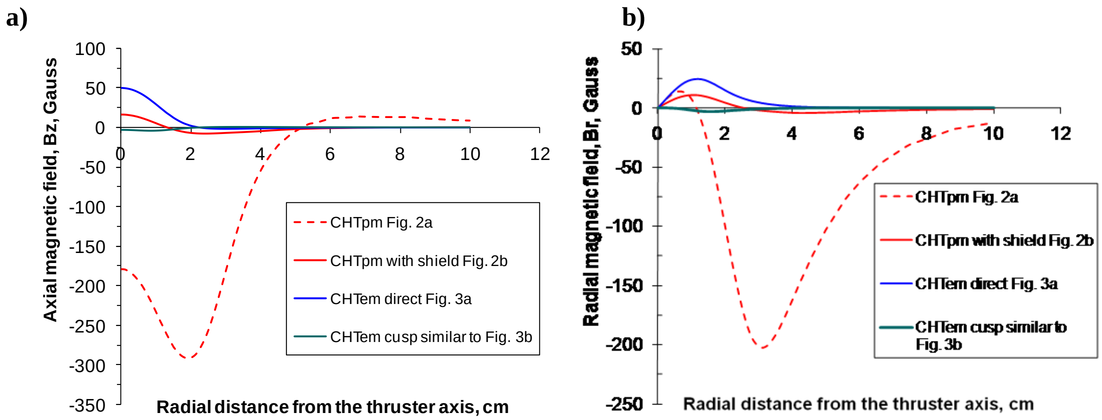

Figure 4. Simulation results of the magnetic field distribution (for the axial (a) and radial (b) components of the magnetic field) in the radial direction at 1 cm from the exit of the 2.6 cm diameter channel of the cylindrical thruster configurations shown in Figs. 2 and 3: CHTpm with and without magnetic shield and CHT with electromagnet coils without the magnetic shield. For the cusp configuration of the CHTem, the front coil current is -2 A and the back coil current is +2.5 A.

cusp magnetic field in the permanent magnet thruster. Finally, the magnetic field outside the permanent magnet thruster is much stronger than the magnetic field outside the CHT with the electromagnet coils (Fig. 4).

The above differences between the magnetic field topologies of the CHTem and CHTpm are due to the differences in the magnetic field produced by current-carrying coils and axially magnetized permanent magnet rings. These differences are discussed in details in Ref. 8. The use of magnetic shield can significantly alter the magnetic field outside the magnetic circuit (Fig. 2b). In fact, for the CHTpm, it allows to greatly reduce the magnetic field outside the magnetic circuit (Fig. 4).

Note that the magnetic field topology produced by a ring-shaped permanent magnet can be approximated by two concentric current-carrying coils of an opposite polarity (See, for example in Ref. 8). This feature was used to design a modified magnetic circuit of the electromagnet CHT thruster with the magnetic shield and an additional shield coil (Figs. 3c and 3d). The magnetic shield is made from the same low carbon steel as the rest of the magnetic core of this thruster. Although this modified magnetic circuit was not optimized, it allowed us to vary the outside magnetic field without significant changes of the magnetic field inside the CHTem thruster. Fig. 5 compares the magnetic field profiles in the axial direction for the relevant shielded and non-shielded configurations of the CHTem at R = 1 cm from the thruster centerline, and the magnetic field profiles in the radial direction at Z = 1 cm from the channel exit. The shield coil current has indeed a small effect on the magnetic field inside the thruster channel (Figs. 5a-b). This is not the case for the magnetic field in the region outside the thruster, which increases with the absolute value of the shield coil current (Figs. 5 c and d).

For the cusp configurations, the magnetic separatrix is placed inside the thruster channel (Figs. 3b and d), while for the direct magnetic field configuration with the magnetic shield, the magnetic separatrix is placed outside the thruster channel (Fig. 3c). In spite of this and other differences between the direct and cusp configurations of the CHTem (Fig. 5), there is at least one common effect of the magnetic shield coil current - it increases the outside magnetic field for both these thruster configurations. In this outside region, the axial component of the magnetic field is much larger than the radial component of the magnetic field (Figs. 5 g and 5h).

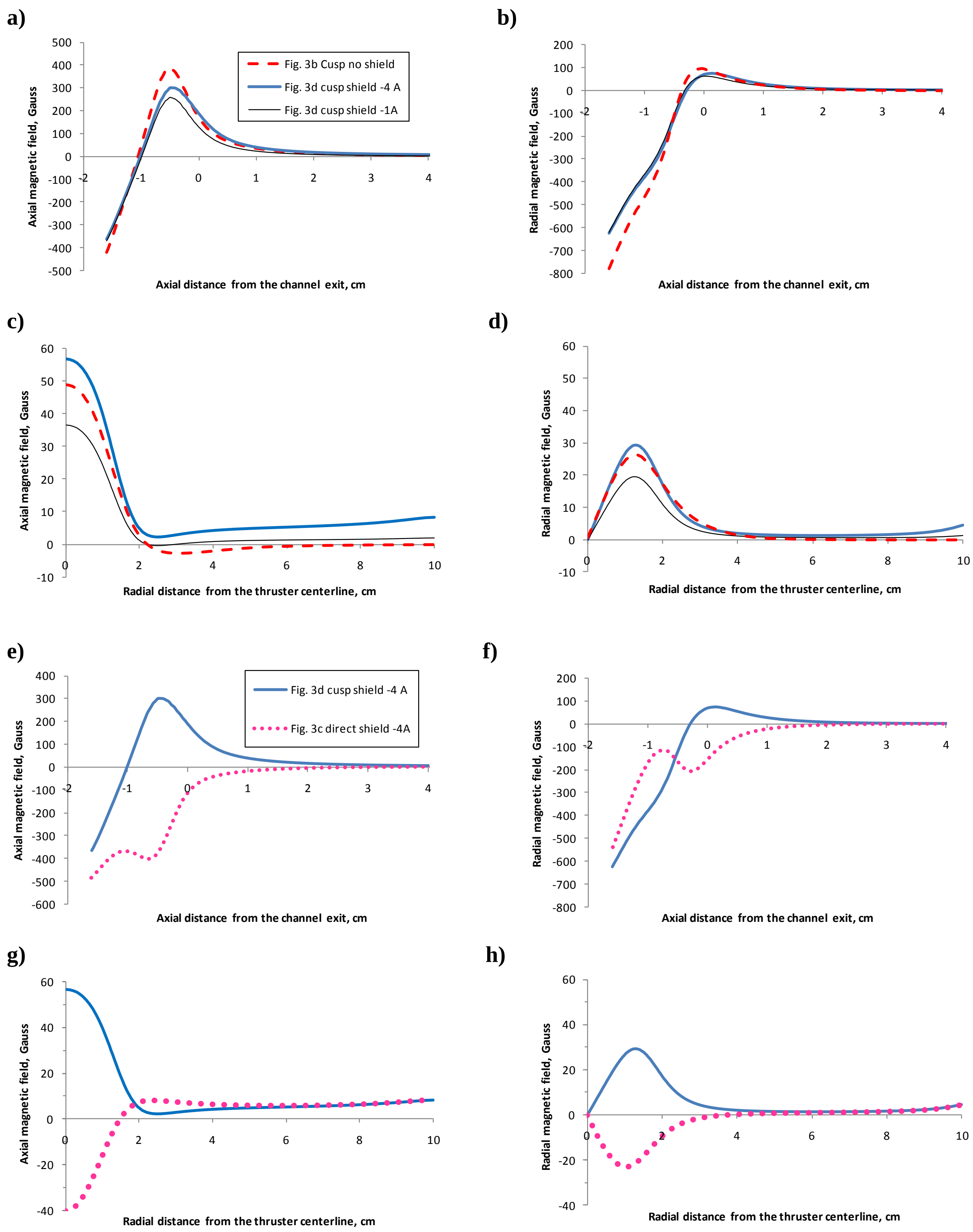

Figure 5. Simulation results of the axial and radial profiles of the magnetic field for the 2.6 cm channel diameter CHTem thruster. The axial profiles along the channel are shown for R = 1 cm from the thruster centerline. The radial profiles are shown at Z = 1 cm from the channel exit. Figures a-d compare the cusp configuration of the CHTem without shield (Fig. 3b) with the shielded configuration of the cusp CHTem (Fig. 3d) at two different shield coil currents: -1 A and -4 A. Figures e-h compares the axial and radial profiles of the magnetic field for two magnetically shielded configurations: direct (Fig. 3c) and cusp (Fig. 3d) at the same shield coil current of -4 A.

III. Experimental setup

In this paper, we present results for the 2.6 cm channel diameter CHTpm and CHTem thrusters. The thruster experiments were conducted in the large PPPL Hall Thruster facility, which consists of a 28 m^3 vacuum vessel equipped with cryopumps.[16] Xenon gas was used in all experiments. For all thrusters used in these experiments, the discharge parameters were: the discharge voltage of 250 V, anode and cathode gas flow rates of 3.5 sccm and 2 sccm, respectively. During the thruster experiments, the background pressure in the vacuum vessel was 1.5 μtorr.

A commercial Heatwave 250 model hollow cathode was used as the cathode-neutralizer. For the magnetically shielded CHTem configurations, the cathode was placed at the distance of 1 cm from the channel exit in the axial direction and about 6 cm from the thruster centerline in the radial direction. For the CHTpm configurations with and without the magnetic shield, we report results for the P2 placement of the cathode (Fig. 2). The cathode keeper electrode was used to initiate the main discharge between the cathode and the thruster anode, and to maintain the discharge current. In the described experiments, the cathode keeper current was 0.5 A during the thruster operation.

The plasma diagnostic tools included a movable floating emissive probe for measurements of the plasma potential at the exit of the thruster channel and the plume probes. The emissive probe was placed on a motorized rotating arm equipped with a potentiometer in order to control and monitor the probe position with respect to the channel exit plane. The plasma potential, ϕ_{pl}, was deduced from measurements of the floating potentials of the hot emissive and cold probes, ϕ_{em}, ϕ_{cold} , respectively,[17,18]

$$\begin{aligned} \phi_{pl} &\approx \phi_{em}^{fl} + 2T_e \\ T_e &\approx \frac{\phi_{em}^{fl} - \phi_{cold}^{fl}}{3.77} \end{aligned} \quad , \qquad (1)$$

where T_e is the electron temperature. In the derivations of Eq. (1), we took into account recent experimental result that the hot emissive probe floats about $2T_e$ below the plasma potential.[18]

In addition, a 2.54 cm diameter guarding ring probe was used to measure the ion angular distribution in the thruster plume.[16] Moreover, a 5 cm diameter bi-directional probe was used to account for the back ion flux from the background plasma.[19] Both probes were biased -30 V with respect to ground in order to collect ions from the plasma plume. The plume probes were suspended on the rotating platform. The distance between the thruster and the planar plume probe was ≈ 73 cm.

IV. Experimental results

A detailed comparison between the discharge and plume characteristics of the CHTpm and CHTem thrusters is described in Refs. 8-11. The most curious difference between results obtained for these thrusters is in the shape of their plumes (Fig. 6). In particular, the CHTpm thrusters produce a halo plume with larger ion flux at larger angles with respect to the axis ~ 30-40° than at the centerline. This shape can change, but still exists at different cathode placements.[3] With the addition of the magnetic shield, the plasma plume acquires a conical shape, which is typical for Hall thrusters.[8,11] Apparently, the magnetically shielded configuration of the CHTpm can produce more focused plasma flow than the CHTem even when both thrusters operate with the auxiliary cathode keeper discharge (in so-called current-overrun regime) (Fig 6).

Plasma potential measurements revealed that for the permanent magnet thruster without the magnetic shield, about 50% of the applied voltage, 250 V, drops outside thruster channel. In this outside region, the magnetic field is strong (200-300 Gauss) and has a strong axial component (Figs. 2a and 4). The use of the magnetic shield reduces the outside magnetic field and causes the acceleration region to shift inside the permanent magnet thruster. For the magnetically shielded configuration of the CHTpm, the outside voltage drop is about 20 % of the applied discharge voltage. These results are comparable with the results of LIF measurements reported in Ref. 9

Fig. 7 compares the results of the plume measurements for the magnetically shielded CHT with electromagnet coils (Figs. 3c and 3d), which were obtained for different values of the shield coil current. In addition, the results for the cusp CHTem without the magnetic shield (Fig. 3b) are also shown on Fig. 7b. For the cusp configuration of the magnetically shielded CHTem, the discharge current changes from 0.89 A to 0.83 A when the shield coil current is varied from zero to – 4 A. For the direct configuration of the magnetically shielded CHTem, the discharge current decreases from 0.63 A to 0.52 A when the shield coil current is varied from zero to -5 A.

According to the results of plume measurements for CHTem without the magnetic shield (Fig. 7b), the presence of the cusp magnetic field with the magnetic separatrix inside the thruster channel (Fig. 3b) does not necessarily lead to the halo shape of the plasma plume. This is unless there is an axial magnetic field outside the thruster channel such as exists for the magnetically shielded configuration of the cusp CHTem (Figs. 3d and 5c). It is suggested that this magnetic field impedes the radial electron flow from the cathode towards the channel exit. The outside magnetic field increases with the shield coil current (absolute value) leading to the depletion of the ion current at the central part of the thruster plume (halo plume).

For the cusp configuration of the CHTem, the currents in the shield and front coils are in the same direction, but opposite to the direction of the current in the back coil. For the direct configuration of the CHTem, the current in the shield coil is opposite to the direction of the currents in both back and front thruster coils (Figs. 3c and 5g). For this thruster configuration, the increase of the shield coil current (absolute value) causes a similar effect on the plasma plume (Fig. 7a) as for the cusp configuration.

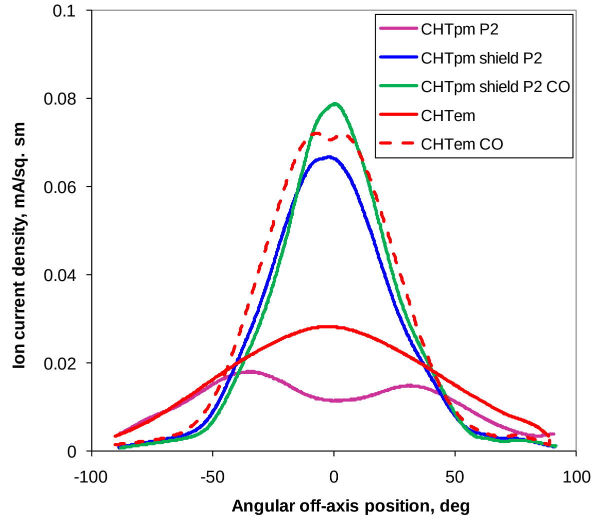

Figure 6. Effect of the magnetic shield on the plasma plume of the CHTpm thruster. The results of the plume measurements for the CHTpm and CHTem thrusters with the auxiliary keeper discharge (so-called current overrun (CO) regime with the keeper current of 2.5 A) are also shown. All thrusters were operated at the discharge voltage of 250 V and Xenon gas flow rate of 3.5 sccm. For the CHTpm thrusters, the cathode placement P2 is shown in Fig. 2.[11] For the CHTem thruster, the cathode placement was different: the cathode outlet orifice was located approximately 5.4 cm away radially and 2 cm downstream from the center of the channel exit.

a)

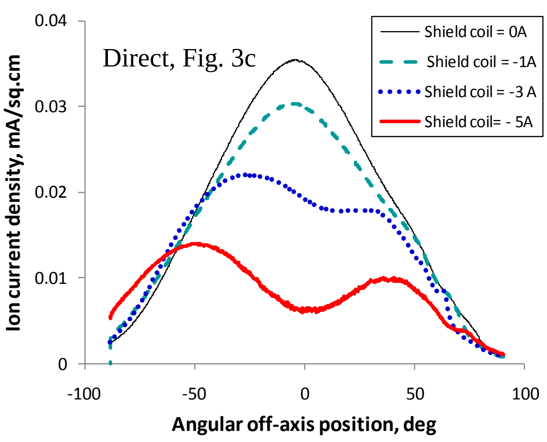

b)

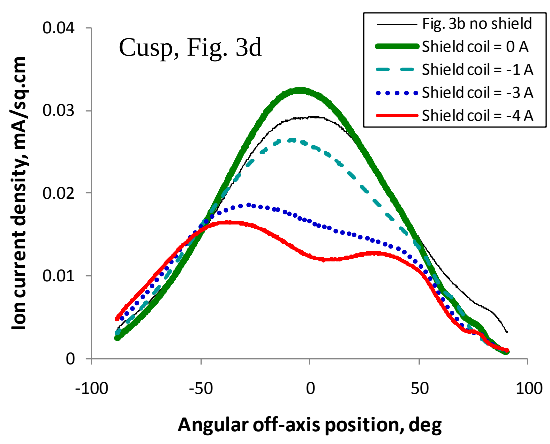

Figure 7. Angular ion current density distribution measured for the shielded CHT thruster with electromagnet coils under variations of the shield coil current: a) direct configuration shown in Fig. 3c and b) cusp configuration shown in Fig. 3d. In addition, the results for the cusp configuration of the CHTem without the magnetic shield and the shield coil (Fig. 3b) are also shown. Fig. 5 compares the magnetic field distribution for some of these thruster configurations. Measurements were conducted for the discharge voltage of 250V, Xenon gas, anode gas flow rate of 3.5 sccm and the cathode gas flow rate of the 2 sccm. For all magnetically shielded CHTem configurations, the cathode was placed at the distance of 1 cm from the channel exit in the axial direction and about 6 cm from the thruster centerline in the radial direction.

Note that for both cusp and direct configurations of the magnetically shielded CHTem, the axial component of the magnetic field at the cathode placement does not exceed 7 Gauss (Fig. 5g) at the shield coil current of -4 A. This is several times larger than the radial component of the magnetic field (Fig. 5h) at the same location. In the radial direction, the distance between the cathode and the channel exit, L, is about 4.5 cm. For a collisionless plasma ($\lambda_e >> L$) outside the thruster, this magnetic field magnitude is enough to impede cathode electrons with the mean energy of ≤ 45 eV on their way to the thruster (i.e. $\omega_{ce}/\nu_e >> 1$ and $L > 2R_{Le}$, where ω_{ce} and ν_e are electron gyrofrequency and collision frequency, respectively, and R_{Le} is the electron gyroradius).

Interesting that for the permanent magnet CHT with the magnetic shield, the cathode placement outside the thruster has an appreciable effect on the thruster discharge and plasma plume.[11] According to Ref. 11, this effect is also associated with the outside magnetic field, which has a similarly small magnitude (~ 5-7 Gauss) as the magnetic field outside the magnetically shielded CHTem at the shield coil current of -4 A (Fig. 5g).

V. Concluding remarks

The presented results support our previous suggestion that for the cylindrical Hall thrusters with permanent magnets, the outside electric and magnetic fields play a critical role in the formation of the plasma flow, including an unusual halo-shape of the plasma plume. Plasma potential measurements revealed that for the CHTpm, a significant part of the acceleration region (~ 50%) is located outside the permanent magnet thruster. In this outside region, the magnetic field is 100-300 Gauss with a stronger axial component than the radial component. The magnitude of this outside magnetic field can be greatly reduced with the addition of the magnetic shield to the magnetic circuit of the permanent magnet thrusters. For the magnetically shielded thruster, the plume has a conic shape, while the outside voltage drop is 20% of the applied discharge voltage. In addition to the change of the plume shape, the use of the magnetic shield causes also a significant plume narrowing. Based on results of experiments with the magnetically shielded configuration of the electromagnet CHT it is suggested that the halo plume occurs when the axial magnetic field outside the thruster impedes the radial electron flow from the cathode to the thruster channel.

Finally, in view of the above results for the CHTpm and CHTem thrusters, and recent results of LIF measurements for the CHTpm thruster[9] and DCF thruster[6], a key fundamental question is to what extent the magnetic field lines are equipotential in these thrusters.

VI. Acknowledgments

The authors wish to thank Martin Griswold, Lee Ellison and Daniel Ruiz of the PPPL for their valuable assistance with experiments. The authors benefited from discussions with Prof. Michael Keidar of the George Washington University, Drs. Slava Spektor, Kevin Diamant and Edward Beiting of the Aerospace Corporation, and Dr. Kurt Polzin of NASA Marshall SFC. This work was supported by the AFOSR.

VII. References

[1] Y. Raitses, Y., and N. J. Fisch, "Parametric Investigations of a Nonconventional Hall Thruster," Phys. Plasmas 8, 2579 (2001).
[2] A. Smirnov, Y. Raitses, and N. J. Fisch, “Experimental and theoretical studies of cylindrical Hall thrusters”, Phys. Plasmas 14, 057106 (2007).
[3] Y. Raitses, E. Merino, J. B. Parker and N. J. Fisch, “Cylindrical Hall thrusters with permanent magnets”, J. Appl. Phys. 108, 093307 (2010).
[4] N. Koch, H. –P. Harmann, G. Kornfeld ” Development and test status of the THALES high efficiency multistage plasma (HEMP) thruster family” Proceedings of the 29th International Electric Propulsion Conference, Princeton, NJ, October 2005, IEPC paper 2005-297.
[5] D. G. Courtney, P. Lozanoy, and M. Martinez-Sanchez., “Continued Investigation of Diverging Cusped Field Thruster”, 44th AIAA/ASME/SAE/ASEE Joint Propulsion Conference & Exhibit, July 2008, Hartford, CT, AIAA paper 2008-4631.
[6] N. A. MacDonald, M. A. Cappelli, S. R. Gildea, M. Martınez-Sanchez and W. A. Hargus Jr, “Laser-induced fluorescence velocity measurements of a diverging cusped-field thruster”, J. Phys. D: Appl. Phys. 44 295203 (2011).
[7] K. A. Polzin, E. S. Sooby, A. C. Kimberlin, Y. Raitses, E. Merino, and N. J. Fisch “Performance of a Permanent-Magnet Cylindrical Hall-Effect Thruster” 45th AIAA/ASME/SAE/ASEE Joint Propulsion Conference, Denver, CO, Aug. 3–5, 2009, AIAA-2009-4812.

[8] Y. Raitses, J. C. Gayoso, E. Merino, and N. J. Fisch, “Effect of the Magnetic Field on the Plasma Plume of the Cylindrical Hall Thruster with Permanent Magnets,” AIAA-2010-6621, the 46th AIAA/ASME/SAE/ASEE Joint Propulsion Conference and Exhibit, Nashville, TN, July 25-28, 2010.

[9] R. Spektor, K. D. Diamant, E.J. Beiting, K. A. Swenson, D..T. Goddard, Y. Raitses and N. J. Fisch, “Characterization of a Cylindrical Hall Thruster with Permanent Magnets” IEPC-2011-264, Proceedings of the 32nd International Electric Propulsion Conference, Wiesbaden, Germany, September 11–15, 2011

[10] K. A. Polzin, Y. Raitses, J. C. Gayoso, and N. J. Fisch, “Comparisons in Performance of Electromagnet and Permanent-Magnet Cylindrical Hall-Effect Thrusters,” AIAA-2010-6695, the 46th AIAA/ASME/SAE/ASEE Joint Propulsion Conference and Exhibit, Nashville, TN, July 25-28, 2010.

[11] J. C. Gayoso, Y. Raitses, and N. J. Fisch, “Cathode Effects on Operation and Plasma Plume of the Permanent Magnet Cylindrical Hall Thruster”, AIAA-2011-5996, the 47th AIAA/ASME/SAE/ASEE Joint Propulsion Conference and Exhibit, San-Diego, CA, August 1-3, 2011. ibid this conference, IEPC paper -2011-264.

[12] Y. Raitses, A. Smirnov, and N.J. Fisch, “Enhanced performance of cylindrical Hall thrusters,” Appl. Phys. Lett. 90, 221502 (2007).

[13] K. D. Diamant, J. E. Pollard, Y. Raitses, and N. J. Fisch, “Ionization, Plume Properties, and Performance of Cylindrical Hall Thrusters,” IEEE Trans. Plasma Sci. 38, 1052 (2010).

[14] A. Smirnov, Y. Raitses, and N. J. Fisch, J. Appl. Phys. **92**, 5673 (2002).

[15] Y. Raitses and N. J. Fisch, “Cylindrical Geometry Hall Thruster,” US Patent No.: 6,448,721 B2, September 2002; Raitses, Y., Fisch, N.J., Ertmer, K.M., and Burlingame, C.A., “A Study of Cylindrical Hall Thruster for Low Power Space Applications,”, 36th Joint Propulsion Conference, Huntsville, AL, July 2000, AIAA paper 2000-3421.

[16] Y. Raitses, D. Staack, A. Dunaevsky, L. Dorf and N. J. Fisch, “Measurements of Plasma Flow in a 2 kW Segmented Electrode Hall Thruster”, in the proceedings of the 28th International Electric Propulsion Conference, Toulouse, France, March 2003, IEPC paper 03-0139.

[17] Y. Raitses, D. Staack, A. Smirnov, and N.J. Fisch, “Space charge saturated sheath regime and temperature saturation in Hall thrusters,” Phys Plasmas 12, 073507 (2005).

[18] J. P. Sheehan, Y. Raitses, N. Hershkowitz, I. Kaganovich, and N. J. Fisch, “A comparison of emissive probe techniques for electric potential measurements in a complex plasma”, Phys. Plasmas, 18, 073501, 2011.

[19] Y. Raitses, T. Moeller and J. Szabo, “AEDC plume measurements using bi-directional ion flux probes”, in the proceedings of the 30th International Electric Propulsion Conference , Florence, Italy, September 2007, IEPC paper 2007-334.